

# Synthesis and Vaccine Evaluation of the Tumor-Associated Carbohydrate Antigen RM2 from Prostate Cancer

Hong-Yang Chuang,<sup>†,‡</sup> Chien-Tai Ren,<sup>†</sup> Chung-An Chao,<sup>†</sup> Chung-Yi Wu,<sup>†</sup> Sachin S. Shivatare,<sup>†,§,‡</sup> Ting-Jen R. Cheng,<sup>†</sup> Chung-Yi Wu,<sup>\*,†</sup> and Chi-Huey Wong<sup>\*,†,‡,‡</sup>

<sup>†</sup>Genomics Research Center, Academia Sinica, 128 Academia Road, Section 2, Nankang, Taipei 115, Taiwan

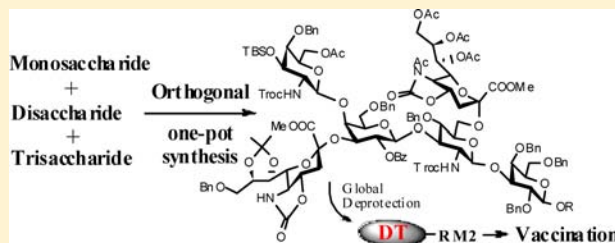
<sup>‡</sup>Department of Chemistry, National Taiwan University, 1 Roosevelt Road, Section 4, Taipei 106, Taiwan

<sup>§</sup>Chemical Biology and Molecular Biophysics, Taiwan International Graduate Program, Academia Sinica, Taipei 115, Taiwan

<sup>\*</sup>Institute of Biochemical Sciences, National Taiwan University, 1 Roosevelt Road, Section 4, Taipei 106, Taiwan

## Supporting Information

**ABSTRACT:** We have successfully developed a [1+2+3] one-pot strategy to synthesize the RM2 antigen hexasaccharide that was proposed to be a prostate tumor antigen. The structure of the synthetic product was verified by NMR analysis and antibody binding assay using a glycan microarray. In addition, the synthetic antigen was conjugated to a mutated diphtheria toxin (DT, CRM197) with different copy numbers and adjuvant combinations to form the vaccine candidates. After vaccination in mice, we used glycan microarrays to monitor their immune response, and the results indicated that, when one molecule of DT was incorporated with 4.7 molecules of RM2 on average (DT-RM<sub>4.7</sub>) and adjuvanted with the glycolipid C34, the combination exhibited the strongest anti-RM2 IgG titer. Moreover, the induced mouse antibodies mediated effective complement-dependent cytotoxicity (CDC) against the prostate cancer cell line LNCap.



## INTRODUCTION

An ideal target antigen for development of cancer vaccine should be specifically expressed on cancer cells and accessible to the immune system. Tumor-associated carbohydrate antigens (TACAs) are not only most abundantly and sometimes aberrantly expressed on the surface of cancer cells but also absent or rarely expressed on normal cells.<sup>1</sup> Many TACAs have been characterized for specific types of cancer<sup>2</sup> and nominated for the development of tumor-specific vaccines.<sup>3,4</sup> However, because carbohydrates generally display poor immunogenicity, a glycan vaccine conjugated with a carrier protein can stimulate the immune response. One example is the Globo H-KLH vaccine, which was first synthesized by Danishefsky and co-workers via the convergent glycal assembly strategy to Keyhole limpet hemocyanin (KLH) conjugate.<sup>5,6</sup> In the phase I clinical trial of Globo H-KLH,<sup>7,8</sup> ~700 (Globo H) GH units conjugated to one KLH protein was administered together with QS21 adjuvant. The treatment appeared to be fairly well-tolerated and was capable of inducing a high titer of IgM antibodies that participate in complement-mediated tumor cell lysis. Currently, this vaccine is in phase III clinical trials in Taiwan and in phase II clinical trials in the United States, Korea, Hong-Kong, and India. Moreover the similar synthetic approaches have been utilized to synthesize other vaccines (e.g., fucosyl-GM1-KLH<sup>9,10</sup> and Le<sup>y</sup>-KLH<sup>11</sup>) against other types of cancer.

In this study, we focused on a novel TACA, the RM2 antigen (Figure 1), a glycosphingolipid (GSL) isolated and identified by

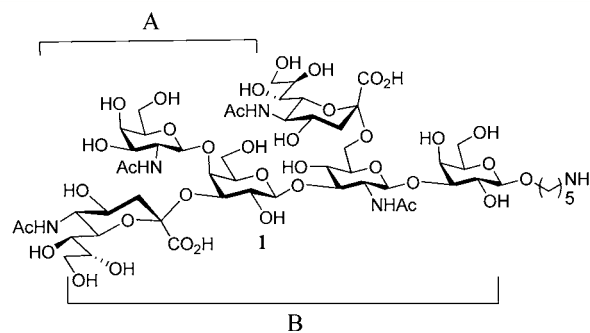


**Figure 1.** The structure of a RM2 carbohydrate hapten 1. (A) Ganglio-series structure. (B) Disialyl lacto-series type-1 structure.

Hakomari and colleagues from a renal cell carcinoma cell line TOS-1 and prostate cancer cell lines LNCap and PC-3.<sup>12</sup> It was immunocharacterized by the monoclonal antibody RM2 and, therefore, termed the “RM2 antigen”. The RM2 antigen,  $\beta$ -1,4-GalNAc-disialyl-Lc, is highly expressed on the prostate cancer cell surface as a glycolipid and possibly as a glycoprotein.<sup>13</sup> In addition, the RM2 antigen expression is closely associated with the prostate cancer staging Gleason grading system and is upregulated as the Gleason grade increases.<sup>14</sup> Therefore, the RM2 antigen can also be developed as a new and novel marker for prostate cancer. The structure of the RM2 antigen consists

Received: April 11, 2013

Published: July 2, 2013

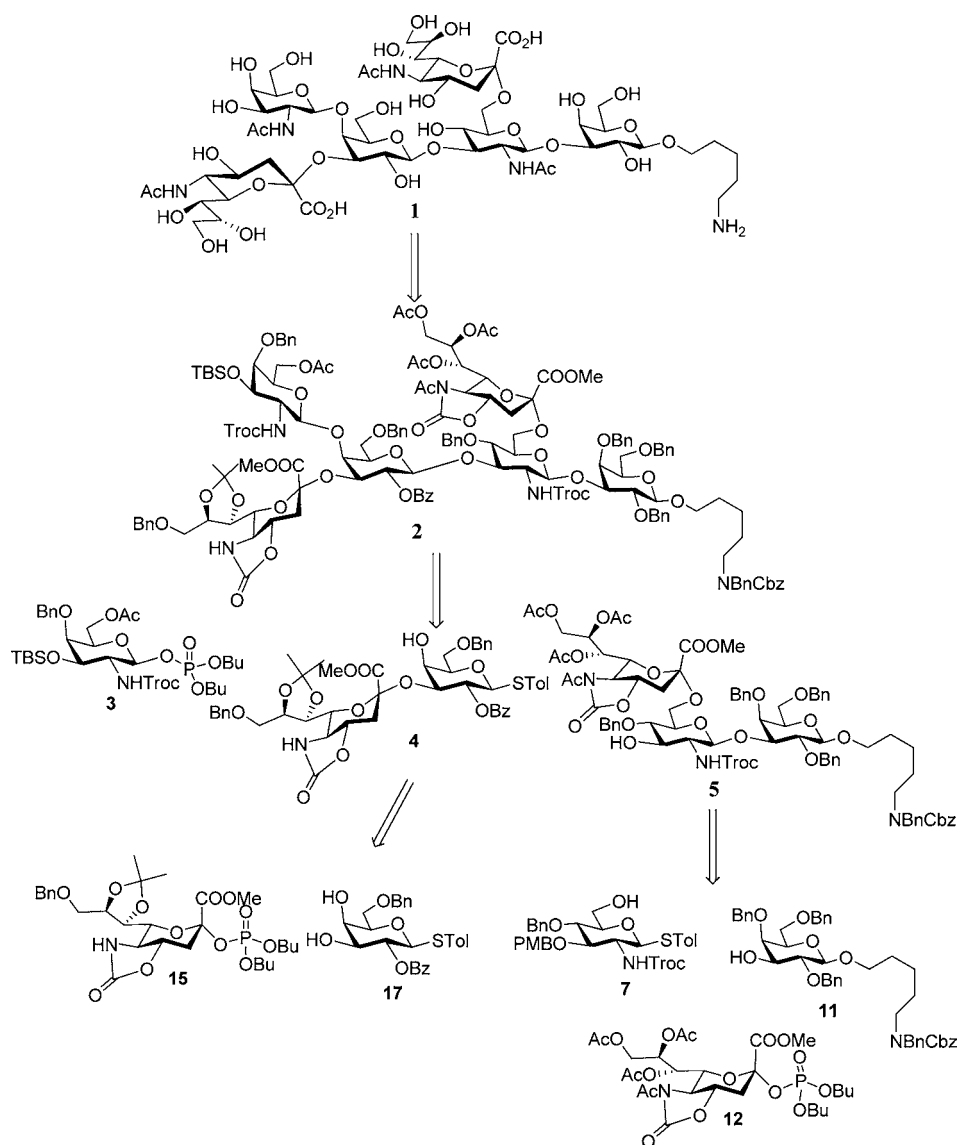


**Figure 2.** Retrosynthetic analysis of the RM2 hapten.

of a novel hybrid core with the “ganglio-series” and the “disialyl lacto-series type 1 chain” groups (Figure 1) and is easily confused with the DSGG antigen, because (1) RM2 and DSGG are indistinguishable on high performance thin-layer chromatography and (2) the renal cell carcinoma expresses many types of disialogangliosides and other globo-series monosialogangliosides, leading to varying proportions of globo-series and ganglio/lacto-series antigens.<sup>15</sup>

On the other hand, this internal hexasaccharide RM2 without the GalNAc residue is identical to  $\alpha(2,3)/\alpha(2,6)$ -disialyl lactotetraose (DSLc4), which was observed as a colon cancer-associated antigen by using a monoclonal antibody (FH9)<sup>16</sup> for siglec-7.<sup>17</sup> Recently, Kiso and co-workers reported a systematic synthesis of DSLc4 via the  $\alpha$ -stereoselective sialylation of O-6 and introduction of the sialyl- $\alpha(2\rightarrow3)$ -D-galactose unit to the O-3 position of GlcNAc.<sup>18</sup>

To further verify the proposed structure of the RM2 antigen, we chemically synthesized the proposed hexasaccharide **1** and evaluated its recognition by monoclonal antibody RM2. To our best knowledge, the RM2 carbohydrate antigen has not been synthesized; the introduction of two sialic acid units to the

compact and rigid 3,4 dibranched galactoside unit is very challenging, due to (1) the presence of the C1 carboxyl group of sialic acids reduces the reactivity of the anomeric position; and (2) the lack of C-3 participating group fails to direct the stereoselectivity and, at the same time, readily promotes the undesired 2,3-elimination. Many approaches have been developed to address these problems, including (1) the design of different leaving groups at the anomeric center;<sup>19–21</sup> (2) the installation of TFA<sup>22</sup> or Troc<sup>23</sup> at the N-5 position; (3) the 1,5-intramolecular lactamization;<sup>24</sup> (4) the use of acetonitrile as solvent in glycosylation;<sup>25</sup> and (5) the installation of 5-N,4,O-carbonyl group (oxazolidinone ring) in sialic acid as a protecting group.<sup>26</sup> Recently, our group incorporated the dibutyl phosphate as leaving group into the N-acetyl-5-N,4-O-carbonyl-protected sialoside as a new sialyl donor to increase  $\alpha$ -selectivity and reaction yield.<sup>27</sup>

Besides the difficulty of sialylation, the development of a method for the  $\beta$ -selective and efficient glycosylation of the galactosamine moiety at the 4-position of dibranched galactose is problematic owing to the steric hindrance of the adjacent sialyl moiety. Here, we describe the use of our sialyl phosphate

as donor to enable an effective synthesis of the hexasaccharide of the proposed RM2 antigen using the [1+2+3] one-pot sequential strategy<sup>28</sup> with high yield and  $\alpha$ -selectivity. The one-pot oligosaccharide synthesis strategy has been recognized as a powerful method to assemble complex oligosaccharides.<sup>29</sup> There are three general one-pot strategies for this purpose: (1) the chemoselective strategy,<sup>28,30,31</sup> (2) the preactivation strategy,<sup>32</sup> and (3) the orthogonal strategy.<sup>33</sup> Although the one-pot synthetic strategy is still needed to build the individual differentially protected building blocks, the major advantage of this method is that the purification of each coupling is not necessary. One just needs to purify the final products after the one-pot reaction. We also synthesized some of the truncated analogues of the proposed RM2 antigen in good yields and stereoselectivity. With these synthetic carbohydrates in hand, we used the RM2 antibody for binding analysis on a glycan array to confirm our synthetic structure. We then conjugated the synthetic RM2 antigen to the carrier protein CRM197 to form the vaccine candidate for vaccination in mice. Glycan arrays were used to monitor the titers of the induced antibody and specificity. We further evaluated the efficacy of the vaccines by CDC assay using the prostate cancer cell line LNCap.

## RESULTS AND DISCUSSION

**Retrosynthesis.** Two main problems in the synthesis of the target compound **1** are encountered:  $\alpha$ -stereo- and regioselective sialylation at O-6 of the GlcNAc residue and O-3 of the Gal residue; and  $\beta$ -selective glycosylation of GalNAc at the O-4 position of the sialyl- $\alpha$ -(2,3)-D-galactose unit.

After careful analysis of the structure of hexasaccharide **1**, we decided to approach the synthesis from a suitably protected hexasaccharide **2** (Figure 2). The hydroxypentamine linker at the reducing end of the galactose residue was designed for immobilizing hexasaccharide **1** onto the NHS-coated slides or conjugating to a carrier protein to form a vaccine candidate. To use the step-by-step protocol for oligosaccharide synthesis, orthogonal protecting groups were required to provide potential acceptor sites for later glycosylation. Overall, the target hexasaccharide can be divided into three parts, monosaccharide **3**,<sup>34</sup> disaccharide **4**, and trisaccharide **5**, which are further divided into six monosaccharide building blocks **3**, **7**, **11**, **12**,<sup>27</sup> **15**, and **17**.

**Synthesis of GlcNAc Building Block 7.** The synthesis of monosaccharide **7** can be achieved from the known 4,6-O-benzylidene acetal **6**<sup>35</sup> (Figure 3). The *p*-methoxybenzylation of

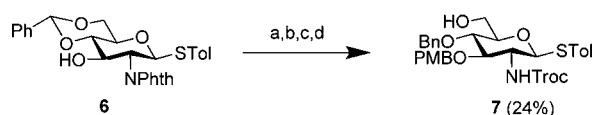


**Figure 3.** Synthesis of GlcNAc building block **7**. (a) NaH, PMBCl, DMF, rt, 1 h. (b)  $\text{BH}_3$ , THF,  $\text{Bu}_2\text{BOTf}$ , 0 °C, 2 h. (c) ethylenediamine, ethanol, 80 °C, 16 h. (d) TrocCl,  $\text{NaHCO}_3$ , THF, rt, 16 h, overall yield 24%.

**6** was carried out by *p*-methoxybenzyl chloride (PMBCl) and sodium hydride (NaH) in DMF, followed by selective ring-opening of the 4,6-O-benzylidene group with dibutylboranetri-flate ( $\text{Bu}_2\text{BOTf}$ ) and borane–tetrahydrofuran complex ( $\text{BH}_3$ , THF). After sequential removal of the phthalimido group and Troc formation, the desired product **7** was produced in four steps in 24% yield.

**Synthesis of Galactose Building Block 11.** The known compound **8**<sup>36</sup> was acetylated by the standard acetylation procedure (Figure 4), and the acetylated compound was

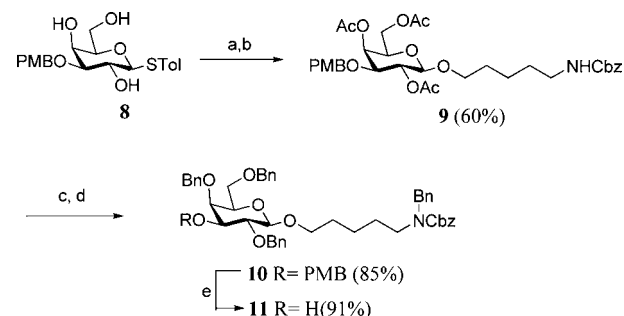


**Figure 4.** Synthesis of galactose building block **11**. (a)  $\text{Ac}_2\text{O}$ , pyridine, rt, 12 h. (b) NIS, cat. TfOH, benzyl 5-hydroxypentylcarbamate,  $\text{CH}_2\text{Cl}_2$ , -30 °C, 3 h, 60% (over two steps). (c) NaOMe, MeOH, rt, 10 h. (d) BnBr, NaH, rt, 2 h, 85% (over two steps). (e) DDQ,  $\text{CH}_2\text{Cl}_2/\text{H}_2\text{O}$ , rt, 2 h, 91%.

glycosylated with the benzyl-5-hydroxypentylcarbamate in dichloromethane using NIS/TfOH as a promoter to afford **9** in 60% yield. Compound **9** was deacetylated under the Zemplén condition; then, benzylation of the triol intermediate afforded **10** in 85% yield. The acetyl group was replaced by the benzyl group to increase the reactivity of the galactose building block, followed by selective removal of the PMB protecting group with DDQ to give **11** in 77% yield.

**Synthesis of Trisaccharide 5.** Compounds **7**, **11**, and **12** were used as starting materials for the synthesis of trisaccharide building block **5** using an orthogonal one-pot synthetic strategy (Figure 5). The one-pot synthetic operation was performed by sialyl phosphate donor **12** (1.5 equiv) and GlcNAc acceptor **7** (1.0 equiv) in the presence of TMSOTf at -60 °C.

The second glycosylation between **7** and **11** was carried out by adding NIS (2.0 equiv) to the reaction solution at higher temperature (-20 °C). Finally, removal of the PMB group by DDQ produced trisaccharide **5** as a single stereoisomer in 42% yield. The configuration of the trisaccharide **5** was examined by NMR spectrometry, and the newly formed  $\alpha$ -glycosidic bond was confirmed by coupling constant  $^3J(\text{C}_1-\text{H}_{3\text{ax}}) = 6.0$  Hz.

**Synthesis of Disaccharide 4.** In order to synthesize the Neu5Aca2→3Gal disaccharide with high  $\alpha$ -stereoselectivity and yield, the thiophenyl group in the anomeric center of 5-*N*,4-*O*-carbonyl-protected thiosialoside **14**<sup>37</sup> was replaced by the dibutyl phosphate group at 0 °C under *N*-iodosuccinimide (NIS) and trifluoromethanesulfonic acid (TfOH) activation for 10 h to obtain **15** in 89% yield ( $\alpha:\beta = 13:1$ ). In addition, compound **16**<sup>36</sup> was efficiently converted to the corresponding 6-*O*-benzyl-4-hydroxy derivative **17** using triethylsilane ( $\text{Et}_3\text{SiH}$ ) and trifluoromethanesulfonic acid (TfOH) in a high yield with excellent regioselectivity. With the 3,4-dihydroxyl galactose acceptor **17** in hand, we first investigated the stereoselectivity of several sialyl phosphate donors including **15** with galactose acceptor **17** to produce Neu5Aca2→3Gal disaccharide (Table S1 in Supporting Information [SI]), and the results showed that the sialyl phosphate donor **15** had the excellent yields and  $\alpha$ -stereoselectivity. The glycosylation of **15** and **17** under the activation of TMSOTf in  $\text{CH}_2\text{Cl}_2$  at -78 °C for 2 h gave Neu5Aca2→3Gal disaccharide **4** as a single isomer in 87% yield (Figure 6). The configuration of the disaccharide **4** was examined by NMR spectrometry, and the new formed  $\alpha$ -

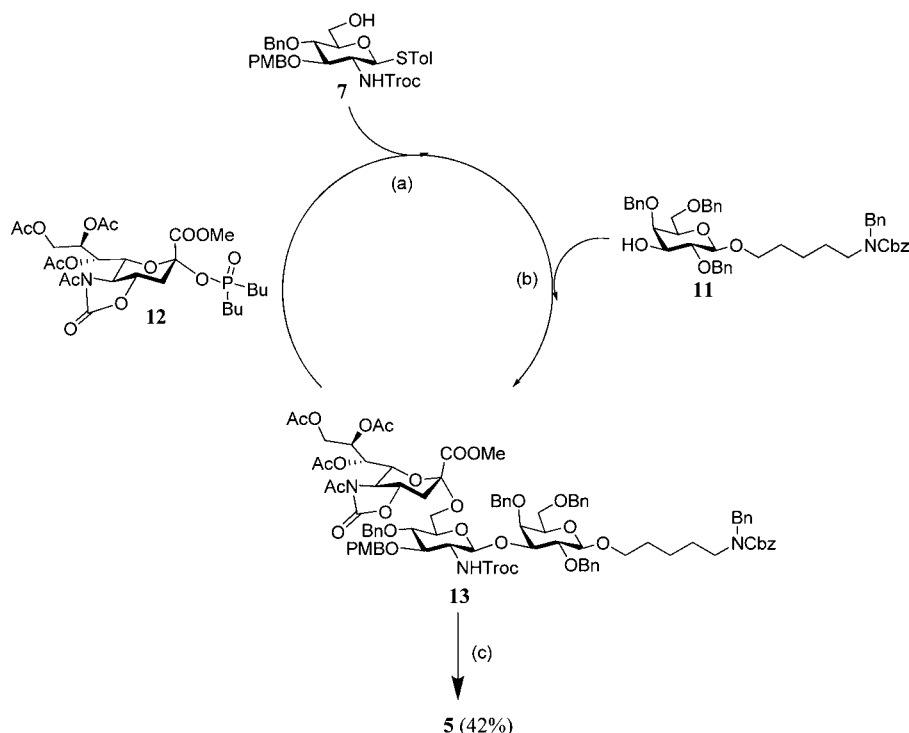


**Figure 5.** Orthogonal one-pot synthesis of trisaccharide **5**. (a) **7**, **12**, TMSOTf, MS 4 Å, CH<sub>2</sub>Cl<sub>2</sub>/CH<sub>3</sub>CN = 1:2, -60 °C, 1 h. (b) **11**, NIS, -20 °C, 2 h. (c) DDQ, CH<sub>2</sub>Cl<sub>2</sub>, H<sub>2</sub>O, rt, 12 h, overall yield 42%.

glycosidic bond was confirmed by coupling constant  $^3J(C_1-H_{3ax}) = 6.1$  Hz.

**Synthesis of Compound 2.** The preparation of the target hexasaccharide **2** was started from the TMSOTf-promoted coupling of the GalNAc donor **3**<sup>34</sup> with disaccharide **4**. After

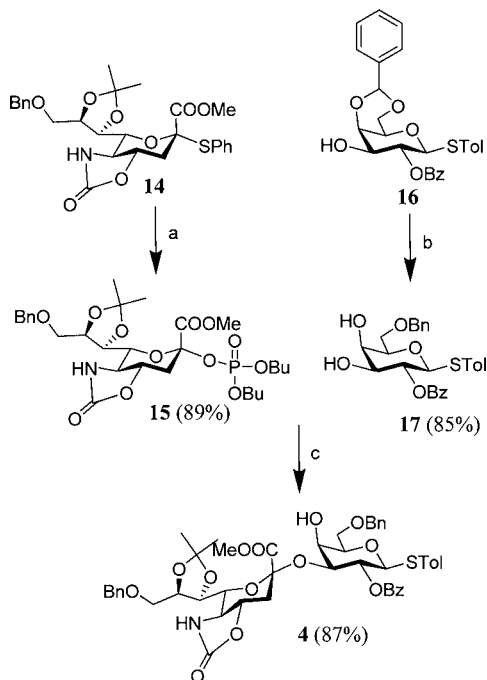


**Figure 6.** Synthesis of disaccharide **4**. (a) NIS, TfOH, dibutylphosphate, MS 4 Å, CH<sub>2</sub>Cl<sub>2</sub>, 0 °C, 10 h, 89%. (b) Et<sub>3</sub>SiH, TfOH, MS 4 Å, CH<sub>2</sub>Cl<sub>2</sub>, -78 °C, 1 h, 85%. (c) TMSOTf, CH<sub>2</sub>Cl<sub>2</sub>, MS 4 Å, -78 °C, 2 h, 87%.

glycosylation, the fully protected trisaccharide compound **18** was isolated in 73% as a 6 to 1 mixture of rotamers (determined by <sup>1</sup>H NMR spectroscopic analysis of the crude reaction). Convergent synthesis of hexasaccharide **2** was achieved as a single stereoisomer in good yield (62%) by glycosylation of trisaccharide acceptor **5** with trisaccharide donor **18** in the NIS/TfOH promoting system at 0 °C for 23 h (Figure 7). We further conducted an orthogonal one-pot [1+2+3] glycosylation and successfully synthesized the target hexasaccharide **2** (Figure 8). Chemoselective glycosylation of the phosphate donor **3** with the thioglycoside **4** under the TBDMSOTf activation in CH<sub>2</sub>Cl<sub>2</sub> at -50 °C provided trisaccharide **18**. Without isolation, the acceptor **5** and NIS were subsequently added to the reaction vessel at 0 °C and the reaction was finished in 23 h to afford the protected hexasaccharide **2** as a single stereoisomer in an overall yield of 32% based on **5**.

**Syntheses of Truncated RM2 Derivatives 20, 22, 24, and 26.** Although RM2 antibody has been reported to recognize the RM2 antigen, its specificity for related carbohydrates is not well studied. To understand the specificity of RM2 antibody, we synthesized the RM2 antigen fragments **27**, **28**, **29**, **30**, and **31** to determine the specificity of monoclonal anti-RM2 antibody. The syntheses of the RM2 fragments **20**, **22**, **24**, and **26** followed the above method (Figure 9). Donors **19**,<sup>38</sup> **21**,<sup>38</sup> or **23**<sup>27</sup> were coupled to acceptor **5** to give tetrasaccharide **20**, pentasaccharide **22**, or pentasaccharide **24**, respectively. In addition, treatment of the trisaccharide donor **18** and disaccharide acceptor **25** with NIS and a catalytic amount of TBDMSOTf at 0 °C gave the protected pentasaccharide **26** in 67% yield.

Global deprotection of the protected hexasaccharide **2** and pentasaccharide **26** was achieved using a four-step procedure: (i) hydrolysis of acyl protecting groups; (ii) acetylation of the amine groups; (iii) removal of the acetonide groups; and (iv)

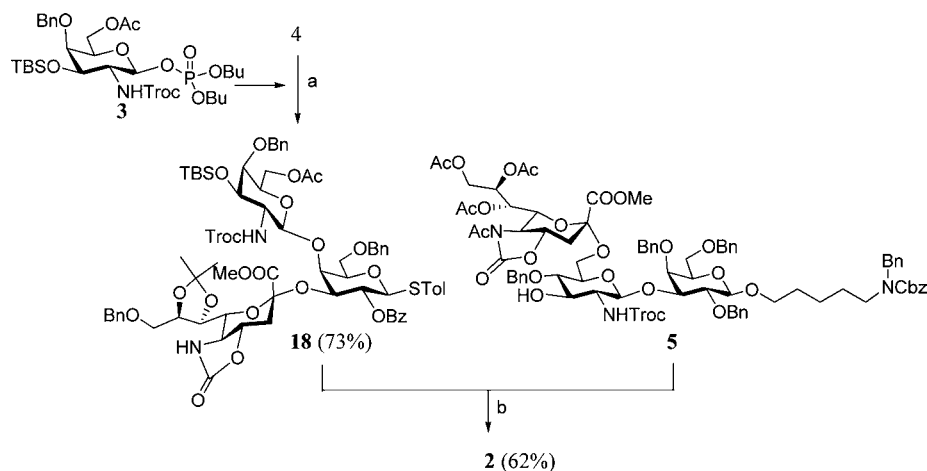


**Figure 7.** Synthesis of hexasaccharide 2. (a) TMSOTf, MS 4 Å, CH<sub>2</sub>Cl<sub>2</sub>, -50 °C, 2 h, 73%. (b) NIS, TfOH, MS 4 Å, CH<sub>2</sub>Cl<sub>2</sub>, 0 °C, 23 h, 62%.

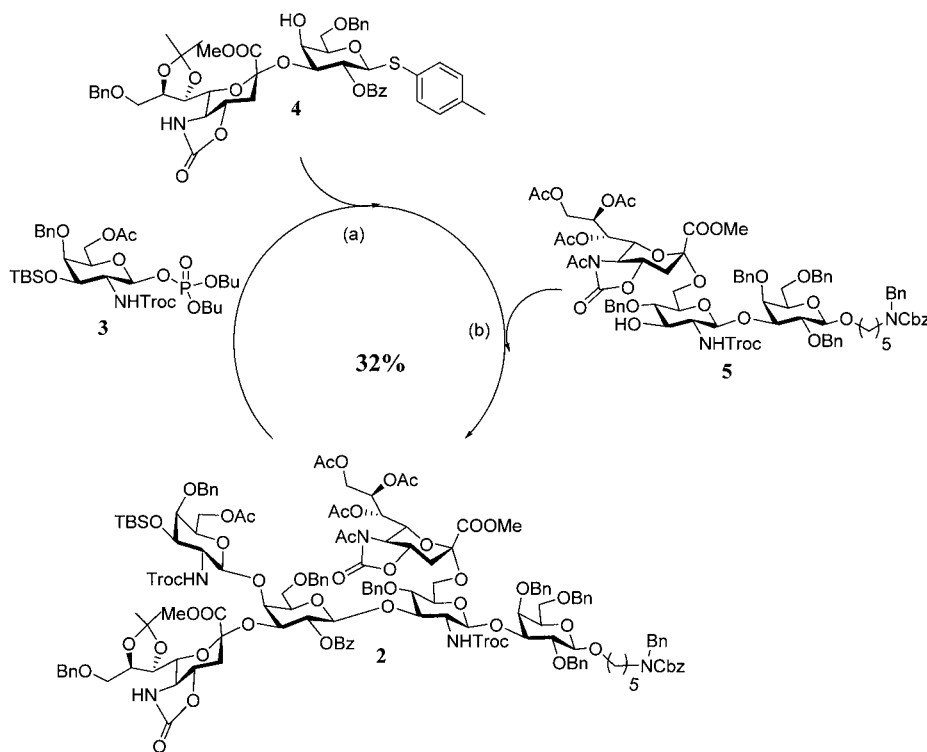


**Figure 8.** One-pot synthesis of hexasaccharide 2. (a) 3, 4, TBDMSOTf, MS 4 Å, CH<sub>2</sub>Cl<sub>2</sub>, -50 °C, 2 h. (b) 5, NIS, 0 °C, 22 h, 32% (over two steps) as a single stereoisomer.

hydrogenolysis of the resulting benzyl ethers to provide the fully deprotected hexasaccharide 1 and pentasaccharide 31. In addition, using a similar strategy, deprotection of 5, 20, 22, and 24 gave the corresponding deprotected oligosaccharides 27–30, respectively, in good yields (Figure 10). These materials can be used for the preparation of a glycan array for antibody binding study and for the preparation of glycoconjugates for vaccine development.

To confirm that the synthesized hexasaccharide 1 was indeed the RM2 antigen and to further understand the antibody binding specificity, we prepared an expanded glycan array containing the synthesized hexasaccharide 1 and its analogues along with the other ninety glycans prepared in our laboratory to from a glycan array for testing (Figure S4 in SI). All glycans were directly immobilized onto NHS-coated glass slides by

taking an aliquot from a stock solution of sugar at a fixed concentration (100 μM). The assay involved an initial treatment with RM2 (a mouse IgM anti-RM2 monoclonal antibody, a kind gift from Prof. Saito), followed by incubation with a mouse fluorescein-tagged IgM secondary antibody against its primary antibody. After one hour incubation, the slides were washed with ddH<sub>2</sub>O twice and scanned to show the binding specificity of the antibody to printed oligosaccharides. The resulting images showed that monoclonal RM2 antibody recognized hexasaccharide 1 specifically, indicating that the synthetic hexasaccharide 1 contains the same antigenic epitope with which RM2 antibody reacts on prostate cancer cells (Figure 11); therefore, we concluded that the synthesized hexasaccharide 1 was indeed the RM2 antigen. Moreover, the structure assignment of the synthesized hexasaccharide 1 is

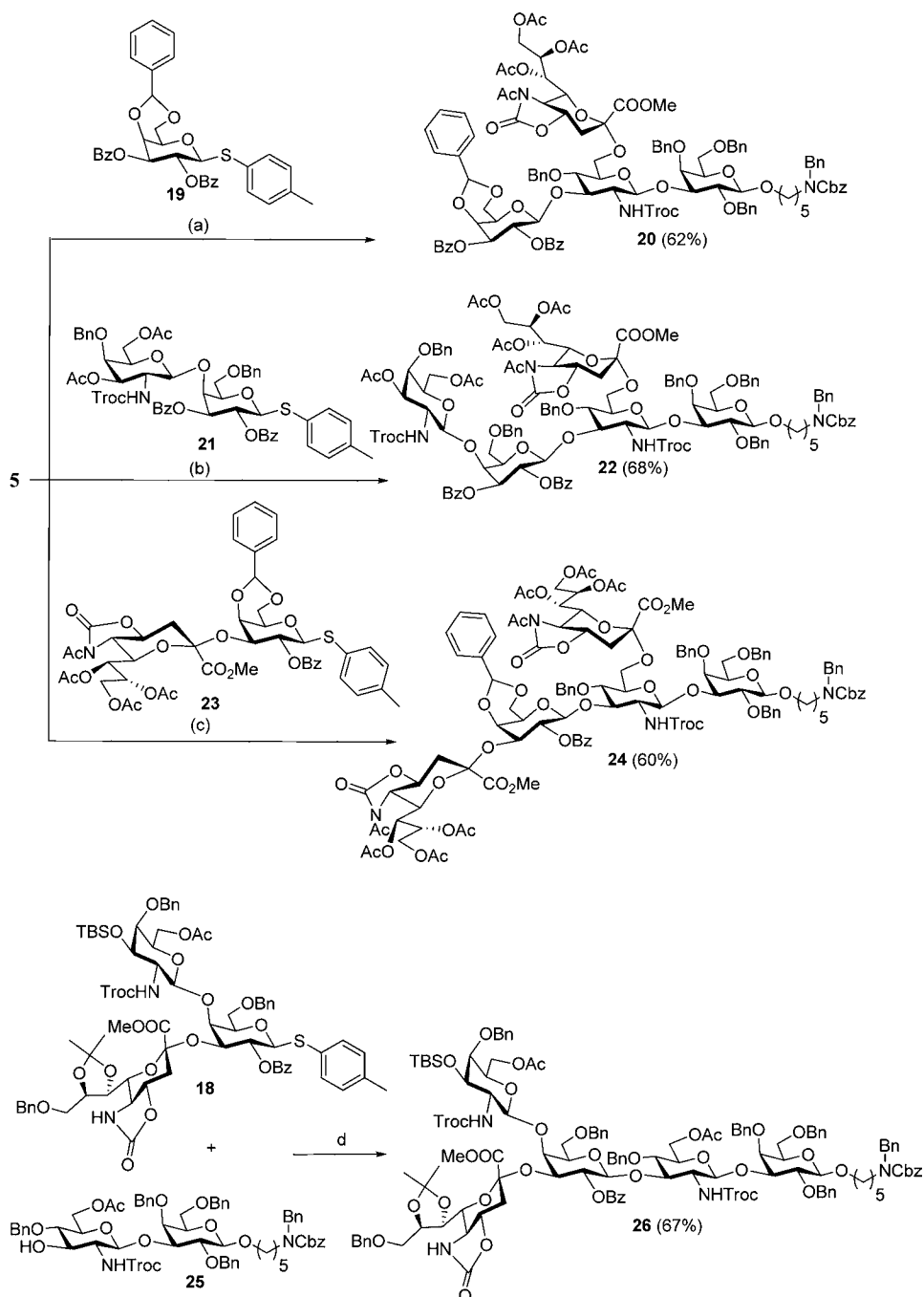


**Figure 9.** Synthesis of **20**, **22**, **24**, and **26**. (a) NIS, TfOH, MS 4 Å, CH<sub>2</sub>Cl<sub>2</sub>, 0 °C, 9 h, 62%. (b) NIS, TfOH, MS 4 Å, CH<sub>2</sub>Cl<sub>2</sub>, 0 °C, 11 h, 68%. (c) NIS, TfOH, MS 4 Å, CH<sub>2</sub>Cl<sub>2</sub>, -20 °C, 3 h, 60%. (d) NIS, TBDMSOTf, MS 4 Å, CH<sub>2</sub>Cl<sub>2</sub>, 0 °C, 8 h, 67%.

confirmed by both 1D- and 2D-NMR (Figure S1 and Table S2 in SI). Furthermore, to determine the dissociation constants of RM2 and truncated analogues on the surface interacting with the antibody in a multivalent manner, we followed the direct measurement method developed in our laboratory,<sup>39</sup> using different concentrations of antibodies and printed sugars. The results showed that, when the printing concentration is below 6.25 μM, the average distance between printed sugars is too far to have enough multivalent effect with antibody RM2. At the printing concentrations from 100 to 6.25 μM, however, we observed that the  $K_{D,surf}$  values measured were narrowly distributed from the individual curves (Figure S2 and Table S3 in SI). Using the same method, the  $K_{D,surf}$  values were

determined for the truncated RM2 analogue **29** interacting with the antibody (Figure S3 and Table S4 in SI). Overall, the relative binding specificity of RM2 for the epitopes was that of RM2 greater than that of pentasaccharide **29** (Table 1).

**Synthesis of DT-RM<sub>4,7</sub> As a Vaccine Candidate with Glycolipid C34 As Adjuvant.** To develop a general protocol<sup>40</sup> for carbohydrate–carrier protein conjugation (Figure 12 and Table S5 in SI), we adopted the thiol-maleimide coupling method for sialic acid-rich compounds. The amine group of the hexasaccharide **1** was reacted with 2 equiv of 3,3'-Dithiobis(sulfosuccinimidylpropionate) (DTSSP) and an amine-reactive *N*-hydroxysulfosuccinimide (sulfo-NHS) ester at each end of an eight-carbon spacer arm in pH 7.4

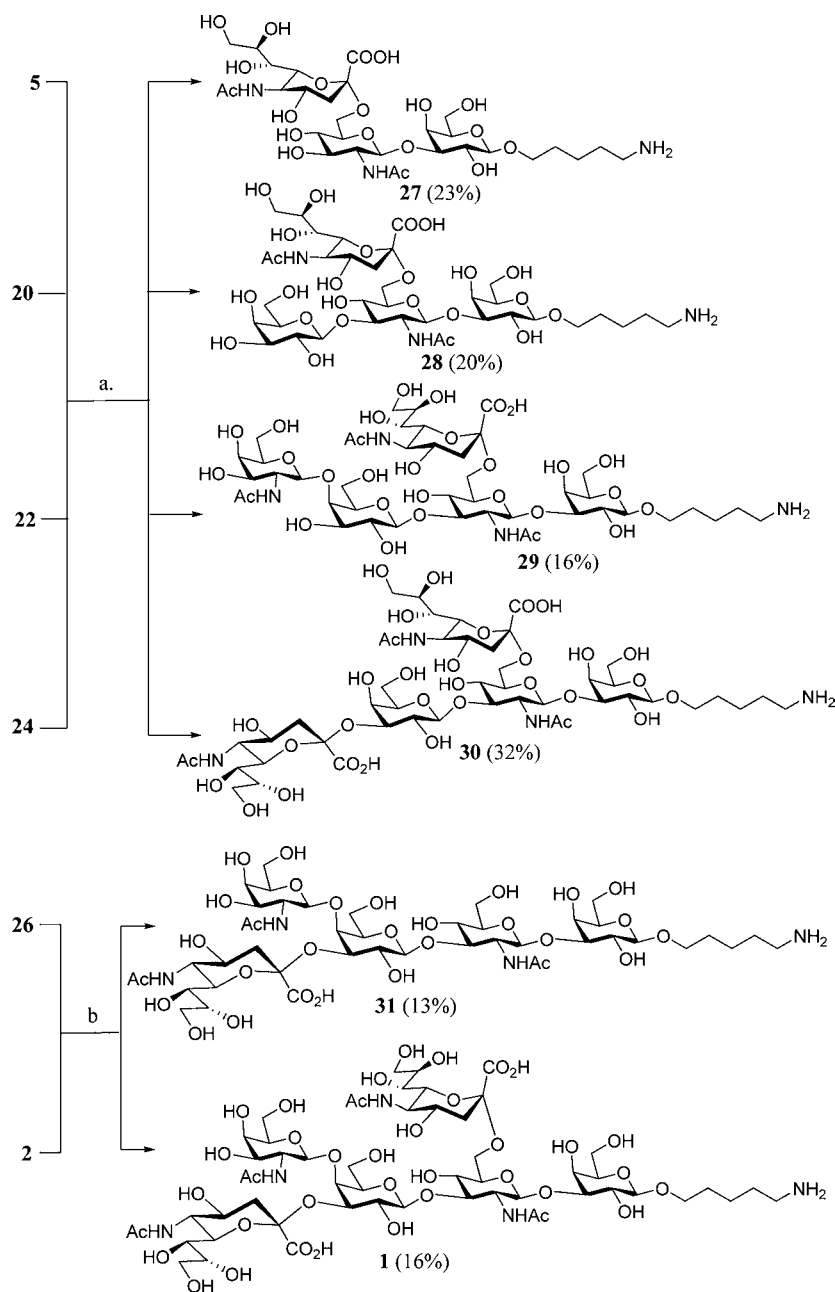


**Figure 10.** Global deprotection of 2, 5, 20, 22, 24, and 26. (a) (i) LiOH·H<sub>2</sub>O, dioxane, H<sub>2</sub>O, 90–95 °C, 36 h; (ii) Ac<sub>2</sub>O, NaHCO<sub>3</sub>, H<sub>2</sub>O then LiOH, H<sub>2</sub>O, rt, 12 h; (iii) Pd(OH)<sub>2</sub>, H<sub>2</sub>, CH<sub>3</sub>OH, H<sub>2</sub>O, rt, 12 h. (b) (i) LiOH·H<sub>2</sub>O, Dioxane, H<sub>2</sub>O, 90–95 °C, 36 h; (ii) Ac<sub>2</sub>O, pyridine, DMAP, 12 h; (iii) BF<sub>3</sub>·OEt<sub>2</sub>, CH<sub>3</sub>CN, 0 °C→rt, 18 h; (iv) LiOH, H<sub>2</sub>O, rt, 12 h (v) Pd(OH)<sub>2</sub>, H<sub>2</sub>, CH<sub>3</sub>OH, H<sub>2</sub>O, rt, 12 h.

phosphate buffer at room temperature for 8 h to afford the corresponding half ester. Next, the disulfide bond was cleaved in the presence of dithiothreitol (DTT) at 40 °C for 2 h to obtain the free thio product **32** as Michael donors in 78% yield after purification on a size exclusion column LH-20. Furthermore, in order to generate the thio-active maleimide group on the protein, CRM197 was reacted with an excess of *N*-( $\epsilon$ -maleimidocaproyloxy)sulfosuccinimide ester (Sulfo-EMCS) in pH 7.0 phosphate buffer for 2 h. The number of molecules of maleimide-linkers on the protein was determined by MALDI-TOF mass spectrometer. In average, 12.85 molecules of maleimide linkers were coupled on each molecule of diphtheria toxin mutant CRM197. Finally, for protein conjugation, the purified thiolated hexasaccharide **32** was incubated with the derivatized protein in pH 7.2 phosphate

buffer for 2 h at room temperature to obtain the RM2 antigen–CRM197 glycoconjugate which was shown to contain 4.7 molecules of RM2 antigen per molecule of CRM197 (DT-RM<sub>4.7</sub>) (Table S3 in SI). Our previous report showed that the glycoconjugate vaccine exhibited a better immunization result to induce a higher IgG titer antibodies when combined with the  $\alpha$ -galactosylceramide analogue C34 as an adjuvant.<sup>30</sup> To study the effect of adjuvant on Ab response, groups of BALB/c mice were immunized intramuscularly with 2  $\mu$ g of DT-RM<sub>4.7</sub> in combination with 2  $\mu$ g of  $\alpha$ -galactosylceramide C1, its analogue C34,<sup>40</sup> or Alu (Figure 13). Three vaccinations were given at two-week intervals. Two weeks after the third injection, sera were collected and subsequently tested with the previously mentioned glycan microarray (96 glycans) (Figure S5 in SI) to estimate the level and diversity of anti-RM2-related antibody.

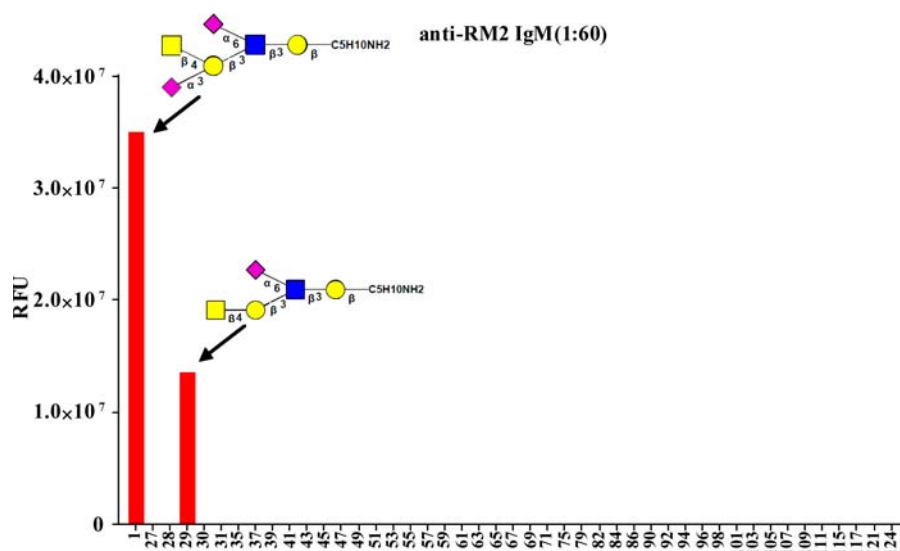


Figure 11. Binding specificity of monoclonal antibodies RM2 to RM2 antigen and its fragments.

Table 1.  $K_{D,surf}$  (nM) Values of Different Antibodies and Different RM2 Analogues

antibody	$K_{D,surf}$ (nM) $\pm$ SD (nM)
RM2 (1)	4.545 $\pm$ 0.903
pentasaccharide (29)	5.756 $\pm$ 1.140

The results showed that mouse anti-RM2 IgG titers increased as vaccination proceeded and peaked after the third vaccination. Among the DT-RM<sub>4,7</sub> vaccinated groups, we found that DT-RM<sub>4,7</sub>/C34 induced higher levels of anti-RM2 IgG titers than did DT-RM<sub>4,7</sub>/C1 or DT-RM<sub>4,7</sub>/Alu after dilution to 12,000-fold (Figure 13).

### Search for the Best Epitope Ratio of DT-RM Vaccine Adjuvanted with C34.

After indentifying C34 as the most effective adjuvant for DT-RM<sub>4,7</sub>, we wanted to determine the best epitope ratio of vaccine by changing the amount of RM2 antigen attached to each carrier protein DT (Figure 13). Various equivalents of thiolated hexasaccharide 32 and different protein concentrations generally would generate diverse carbohydrate–protein ratios. The number of RM2 antigens on the protein was determined by MALDI-TOF mass spectrometry. After dialysis and analysis, we were able to conjugate, on average, 1.0, 3.0, 4.7, and 10 molecules of RM2 antigen to one molecule DT to give DT-RM<sub>1,0</sub>, DT-RM<sub>3,0</sub>, DT-RM<sub>4,7</sub>, and DT-RM<sub>10,0</sub> (Table S5 in SI). Using the same

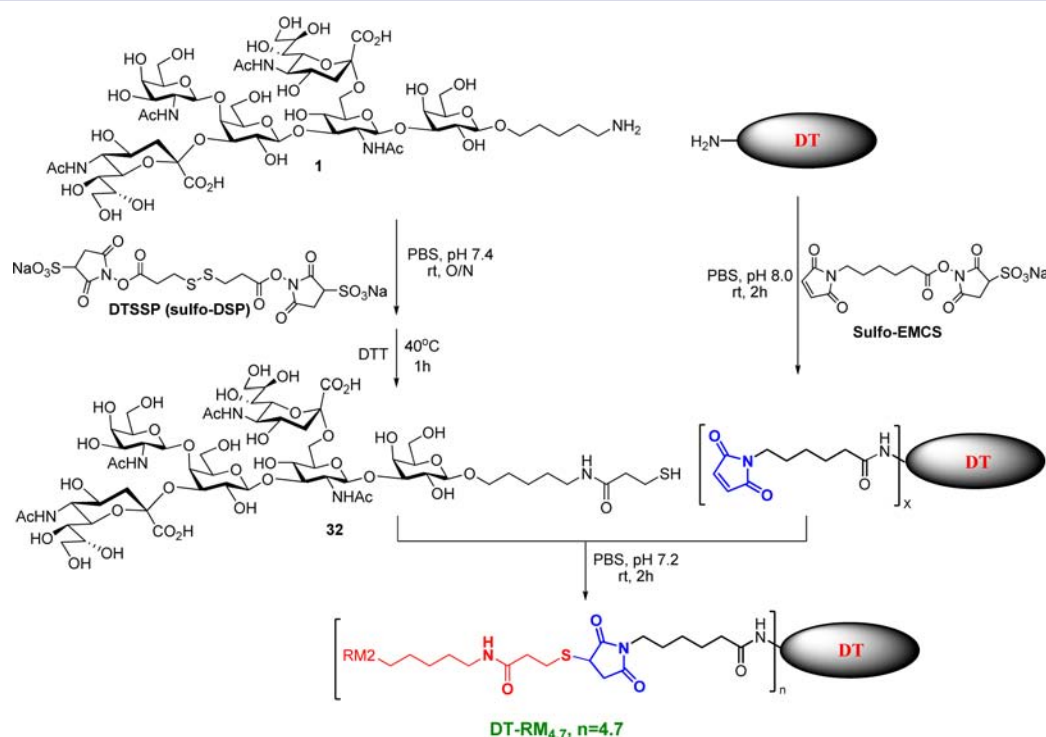
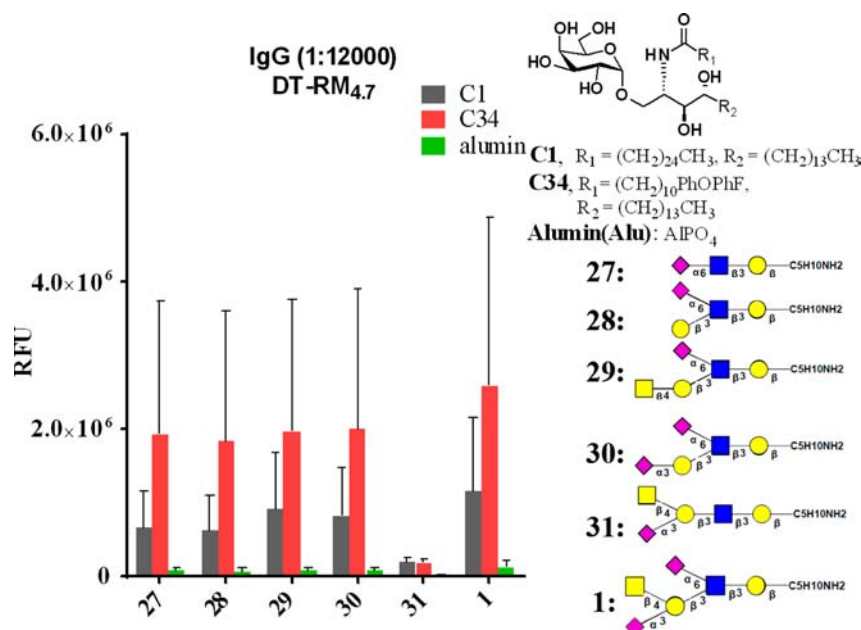


Figure 12. Scheme for producing synthetic candidate carbohydrate-based vaccine.





**Figure 13.** Female BALB/c mice were immunized with 2  $\mu$ g of RM2 antigen of DT-RM<sub>4,7</sub> in combination with 2  $\mu$ g of C1, C34, or Alu. Mouse serum was collected two weeks after the final immunization, and the production of IgG against RM2 antigen and its truncated analogues after dilution to 12,000-fold was measured. Data represent total fluorescence intensity of five mice  $\pm$  the SEM.

vaccination protocol mentioned previously, sera were collected 2 weeks after the third vaccination, and the elicited Abs were subsequently profiled by an RM2-coated glycan microarray. In general, we observed that, when mice were immunized with DT-RM<sub>3,0</sub> alone without adjuvant, only low titers of anti-RM2 IgG (Figure S4A in SI) were generated. The glycan microarray results showed that, on average, 4.7 RM2 antigens conjugated to one DT induced the most abundant IgG titers against RM2 (Figure 14 and Figure S4 in SI). Alternatively, when mice were

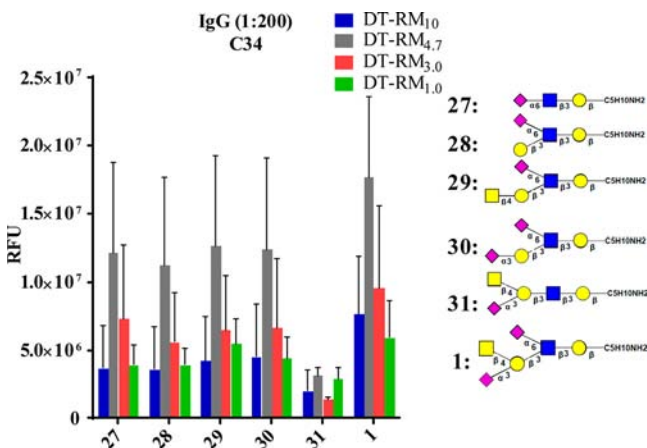


**Figure 14.** Induced IgG titers against RM2 antigen and glycan binding profile of IgG collected from different epitope ratios of DT-RM/C34-immunized mice.

immunized with DT-RM<sub>3,0</sub> alone without adjuvant, only low titers of anti-RM2 IgG (Figure S4A in SI) were generated. When we fixed the signal-to-noise (S/N) ratio to be  $>3$ , the induced IgG could be diluted to 12,000-fold before the signal disappeared (Figure S4F in SI). However, the induced IgM titer could only be diluted to 60-fold (Figure S4E in SI), and the

IgM signals reached background levels after dilution to 200-fold.

Interestingly, the specificity analysis of the induced IgG antibodies by DT-RM<sub>4,7</sub>/C34 vaccine showed that the induced antibodies had a strong binding to the RM2 antigen and weaker binding to its trisaccharide 27, tetrasaccharide 28, pentasaccharide 29, and pentasaccharide 30 epitopes (Figure 14). We observed that these oligosaccharides all contain the same epitope trisaccharide 27 (NeuAca2 $\rightarrow$ 6GlcNAc $\beta$ 1 $\rightarrow$ 3Gal $\beta$ 1 $\rightarrow$ R). To further evaluate the vaccine specificity, we constructed a glycan microarray created by STn, DSGG, RM2 antigen, RM2 antigen analogues, and RM2 antigen fragments (Figure 15). In general, specificity analysis of the induced antibodies by DT-RM<sub>4,7</sub>/C34 vaccine showed that the induced antibodies mainly

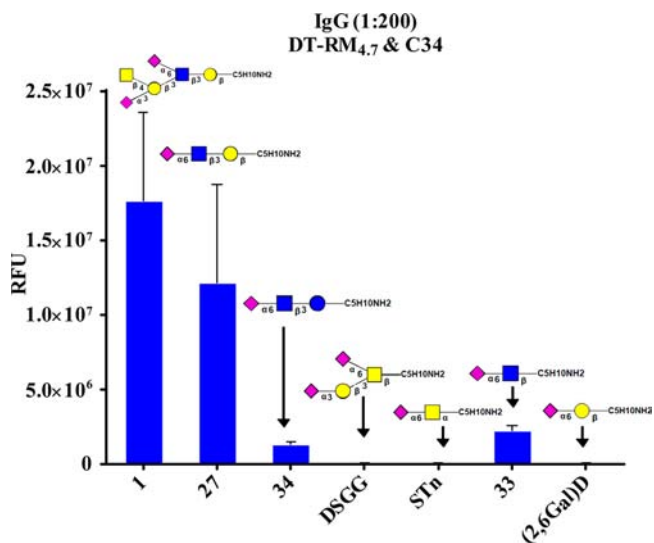


**Figure 15.** Specificity analysis of the induced antibodies by DT-RM<sub>4,7</sub>/C34 vaccine.

bound to the RM2 antigen and to its trisaccharide epitope 27 but at a lesser extent to disaccharide 32 (NeuAc $\alpha$ 2 $\rightarrow$ 6GlcNAc $\beta$ 1 $\rightarrow$ R) and trisaccharide 33 (NeuAc $\alpha$ 2 $\rightarrow$ 6GlcNAc $\beta$ 1 $\rightarrow$ 3Glu $\beta$ 1 $\rightarrow$ R). In addition, there is no detectable signal of binding to NeuAc $\alpha$ 2 $\rightarrow$ 6Gal, DSGG, or STn.

It was reported that DT could induce antigen-specific T cell proliferation and elevate splenocyte production of IL-2, IFN- $\gamma$ , and IL-6, suggesting their role in the Th1 driven pathway.<sup>41–43</sup> Furthermore, the glycolipid C34 was able to induce higher production of IFN- $\gamma$  and IL-4, indicating a more Th1-skewed antigen.<sup>44</sup> However, the anti-DT-RM<sub>4,7</sub>/C34 antibodies of the induced subtypes were mainly IgG1 antibodies with a trace amount of IgG2b and IgG2c antibodies and no detectable IgG2a (Figure 16).

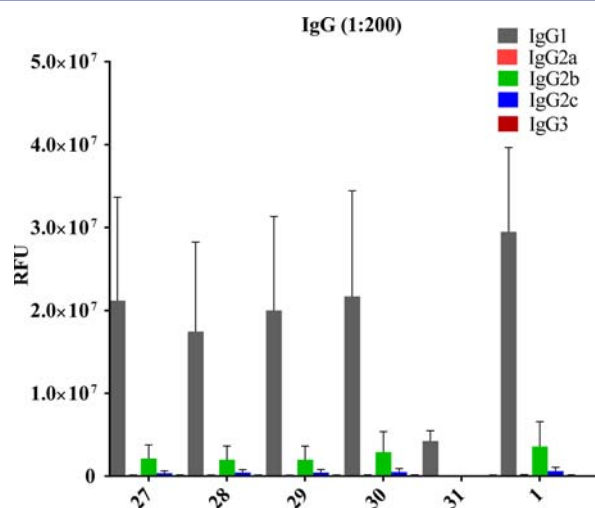


**Figure 16.** Glycan binding profiles of the induced IgG subtypes of the titers collected from DT-RM<sub>4,7</sub>/C34-immunized mice two weeks after the third injection.

Complement-dependent cytotoxicity (CDC) is one of the most potent cell-killing mechanisms mediating the immune response in which IgG or IgM antibodies bind to antigens on the tumor or cancer cell surface. Complement activation, initiated through complement protein C1q binding to the Fc region of the IgM- or IgG-isotype antibody, represents the important activity of antibodies against circulating tumor cells and micrometastases. To evaluate the therapeutic potential of anti-RM2 antibodies, we tested the complement-dependent cytotoxicity with prostate cancer cell line LNCap in the presence of new-born rabbit complement. The ability of antibodies to induce complement activation is strongly dependent on the antibody isotype and the epitope recognized. Thus, isotypes IgG1 and IgG3 are able to activate the complement cascade particularly well through C1q, in contrast to IgG2 and IgG4.<sup>45</sup> As shown in Figure 16, our vaccine formulation resulted in a higher titer of subclass IgG1 antibodies than of other subclasses, and the immune serum showed a strong complement-mediated cytotoxic activity on the RM2-positive human prostate cancer cell line LNCap (Figure 17). These data suggested that our carbohydrate-based vaccine, DT-RM, based on the chemically synthetic hexaccharide 1 and a mutated diphtheria toxin (DT) with adjuvant C34 may create an efficient immune stimulation in human.

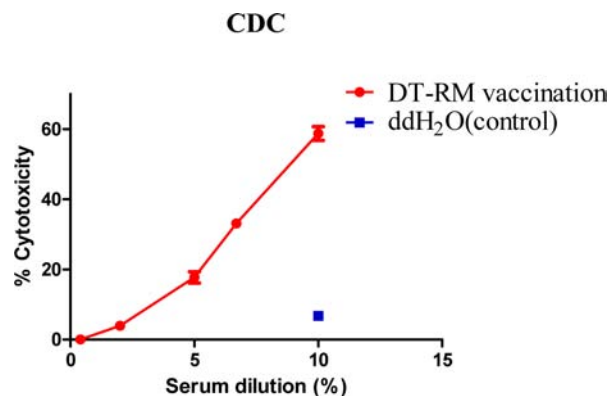


**Figure 17.** CDC activity of the induced antibodies by serum from vaccination mice in the presence of rabbit complement. Lysis of human prostate cancer cell line LNCap at different concentrations.

## CONCLUSION

In conclusion, we have successfully synthesized the prostate tumor carbohydrate RM2 antigen and its analogues as single stereoisomers in every glycosylation step in good yields. We used these synthetic glycans combined with other related glycans to form a 96-member glycan microarray to study the specificity of monoclonal RM2 antibody and confirmed the structure of our synthetic RM2 hexasaccharide antigen. Moreover, the synthesized RM2 carbohydrate antigen was incorporated into the carrier protein CRM197 in an average number of 1–10. After vaccination studies in mice, we used the glycan microarray to monitor their immune response. Our results indicated that, when one molecule of DT was conjugated with 4.7 molecules of RM2 antigen in average (DT-RM<sub>4,7</sub>) and adjuvanted with the glycolipid C34, the strongest anti-RM2 antigen titer was exhibited. More importantly, these oligosaccharide–protein conjugates are TD antigens, and the induced IgG antibody titers were much higher than IgM antibody titers. In IgG subclasses analysis, IgG1 antibody was predominant in the serum, while IgG3, a typical anti-carbohydrate antibody, was also present in high level. In addition, the induced mouse antibodies mediated effective complement-dependent cytotoxicity (CDC) against the prostate cancer cell line LNCap.

## ASSOCIATED CONTENT

### Supporting Information

Supplementary schemes, synthetic methods, and experimental protocols. This material is available free of charge via the Internet at <http://pubs.acs.org>.

## AUTHOR INFORMATION

### Corresponding Author

cyiwu@gate.sinica.edu.tw; ch Wong@gate.sinica.edu.tw

### Notes

The authors declare no competing financial interest.

## ACKNOWLEDGMENTS

We thank Prof. Seiichi Saito at the University of the Ryukyus, Okinawa, Japan, for kindly providing RM2 antibody, and Dr. Kun-Hsien Lin for providing the adjuvant C34. This work was supported by Academia Sinica and National Science Council, Taiwan. (Grants NSC-100-2325-B-001-015 and NSC-101-2325-B-001-014 to C.-Y.W.).

## ■ REFERENCES

- (1) Stevanovic, S. *Nat. Rev. Cancer* **2002**, *2*, 514.
- (2) Hakomori, S.; Zhang, Y. M. *Chem. Biol.* **1997**, *4*, 97.
- (3) Freire, T.; Bay, S.; Vichier-Guerre, S.; Lo-Man, R.; Leclerc, C. *Mini-Rev. Med. Chem.* **2006**, *6*, 1357.
- (4) Dube, D. H.; Bertozzi, C. R. *Nat. Rev. Drug Discovery* **2005**, *4*, 477.
- (5) Ragupathi, G.; Park, T. K.; Zhang, S. L.; Kim, I. J.; Graber, L.; Adluri, S.; Lloyd, K. O.; Danishefsky, S. J.; Livingston, P. O. *Angew. Chem., Int. Ed.* **1997**, *36*, 125.
- (6) Park, T. K.; Kim, I. J.; Hu, S. H.; Bilodeau, M. T.; Randolph, J. T.; Kwon, O.; Danishefsky, S. J. *J. Am. Chem. Soc.* **1996**, *118*, 11488.
- (7) Slovin, S. F.; Ragupathi, G.; Adluri, S.; Ungers, G.; Terry, K.; Kim, S.; Spassova, M.; Bornmann, W. G.; Fazzari, M.; Dantis, L.; Olkiewicz, K.; Lloyd, K. O.; Livingston, P. O.; Danishefsky, S. J.; Scher, H. I. *Proc. Natl. Acad. Sci. U.S.A.* **1999**, *96*, 5710.
- (8) Gilewski, T.; Ragupathi, G.; Bhuta, S.; Williams, L. J.; Musselli, C.; Zhang, X. F.; Bornmann, W. G.; Spassova, M.; Bencsath, K. P.; Panageas, K. S.; Chin, J.; Hudis, C. A.; Norton, L.; Houghton, A. N.; Livingston, P. O.; Danishefsky, S. J. *Proc. Natl. Acad. Sci. U.S.A.* **2001**, *98*, 3270.
- (9) Nagorny, P.; Kim, W. H.; Wan, Q.; Lee, D.; Danishefsky, S. J. *J. Org. Chem.* **2009**, *74*, 5157.
- (10) Dickler, M. N.; Ragupathi, G.; Liu, N. X.; Musselli, C.; Martino, D. J.; Miller, V. A.; Kris, M. G.; Brezicka, F. T.; Livingston, P. O.; Grant, S. C. *Clin. Cancer Res.* **1999**, *5*, 2773.
- (11) Sabbatini, P. J.; Kudryashov, V.; Ragupathi, G.; Danishefsky, S. J.; Livingston, P. O.; Bornmann, W.; Spassova, M.; Zatorski, A.; Spriggs, D.; Aghajanian, C.; Soignet, S.; Peyton, M.; O'Flaherty, C.; Curtin, J.; Lloyd, K. O. *Int. J. Cancer* **2000**, *87*, 79.
- (12) Yamago, S.; Yamada, T.; Hara, O.; Ito, H.; Mino, Y.; Yoshida, J. *Org. Lett.* **2001**, *3*, 3867.
- (13) Saito, S.; Murayama, Y.; Pan, Y.; Taima, T.; Fujimura, T.; Murayama, K.; Sadilek, M.; Egawa, S.; Ueno, S.; Ito, A.; Ishidoya, S.; Nakagawa, H.; Kato, M.; Satoh, M.; Endoh, M.; Arai, Y. *Int. J. Cancer* **2008**, *123*, 633.
- (14) Saito, S.; Egawa, S.; Endoh, M.; Ueno, S.; Ito, A.; Numahata, K.; Satoh, M.; Kuwano, S.; Baba, S.; Hakomori, S.; Arai, Y. *Int. J. Cancer* **2005**, *115*, 105.
- (15) Ito, A.; Saito, S.; Masuko, T.; Oh-eda, M.; Matsuura, T.; Satoh, M.; Nejad, F. M.; Enomoto, T.; Orikasa, S.; Hakomori, S. *Glycoconjugate J.* **2001**, *18*, 475.
- (16) Fukushi, Y.; Nudelman, E.; Levery, S. B.; Higuchi, T.; Hakomori, S. *Biochemistry* **1986**, *25*, 2859.
- (17) Ito, A.; Handa, K.; Withers, D. A.; Satoh, M.; Hakomori, S. I. *FEBS Lett.* **2001**, *504*, 81.
- (18) Ando, T.; Ishida, H.; Kiso, M. *Carbohydr. Res.* **2003**, *338*, 503.
- (19) Brown, D. A.; Kondo, K. L.; Wong, S. W.; Diamond, D. J. *Eur. J. Immunol.* **1992**, *22*, 2419.
- (20) Marra, A.; Dong, X.; Petitou, M.; Sinay, P. *Carbohydr. Res.* **1989**, *195*, 39.
- (21) Haberman, J. M.; Gin, D. Y. *Org. Lett.* **2003**, *5*, 2539.
- (22) Lin, C. C.; Huang, K. T. *Org. Lett.* **2005**, *7*, 4169.
- (23) Ando, T.; Ishida, H.; Kiso, M. *Carbohydr. Res.* **2003**, *338*, 503.
- (24) Ando, H.; Koike, Y.; Koizumi, S.; Ishida, H.; Kiso, M. *Angew. Chem., Int. Ed.* **2005**, *44*, 6759.
- (25) Crich, D.; Li, W. J. *Org. Chem.* **2007**, *72*, 7794.
- (26) Tanaka, H.; Nishiura, Y.; Takahashi, T. *J. Am. Chem. Soc.* **2006**, *128*, 7124.
- (27) Hsu, C. H.; Chu, K. C.; Lin, Y. S.; Han, J. L.; Peng, Y. S.; Ren, C. T.; Wu, C. Y.; Wong, C. H. *Chem.—Eur. J.* **2010**, *16*, 1754.
- (28) Raghavan, S.; Kahne, D. J. *J. Am. Chem. Soc.* **1993**, *115*, 1580.
- (29) Hsu, C. H.; Hung, S. C.; Wu, C. Y.; Wong, C. H. *Angew. Chem., Int. Ed.* **2011**, *50*, 11872.
- (30) Ley, S. V.; Priepke, H. W. M. *Angew. Chem., Int. Ed.* **1994**, *33*, 2292.
- (31) Ley, S. V.; Priepke, H. W. M.; Warriner, S. L. *Angew. Chem., Int. Ed.* **1994**, *33*, 2290.
- (32) Crich, D.; Sun, S. X. *J. Am. Chem. Soc.* **1998**, *120*, 435.
- (33) Kanie, O.; Ito, Y.; Ogawa, T. *J. Am. Chem. Soc.* **1994**, *116*, 12073.
- (34) Komori, T.; Imamura, A.; Ando, H.; Ishida, H.; Kiso, M. *Carbohydr. Res.* **2009**, *344*, 1453.
- (35) Huang, L. J.; Wang, Z.; Li, X. N.; Ye, X. S.; Huang, X. F. *Carbohydr. Res.* **2006**, *341*, 1669.
- (36) Wang, Z.; Zhou, L. Y.; El-Boubbou, K.; Ye, X. S.; Huang, X. F. *J. Org. Chem.* **2007**, *72*, 6409.
- (37) Tanaka, H.; Nishiura, Y.; Takahashi, T. *J. Am. Chem. Soc.* **2008**, *130*, 17244.
- (38) Lu, G. K.; Wang, P.; Liu, Q. C.; Zhang, Z. H.; Zhang, W.; Li, Y. X. *Chin. J. Chem.* **2009**, *27*, 2217.
- (39) Liang, P. H.; Wang, S. K.; Wong, C. H. *J. Am. Chem. Soc.* **2007**, *129*, 11177.
- (40) Huang, Y. L.; Hung, J. T.; Cheung, S. K.; Lee, H. Y.; Chu, K. C.; Li, S. T.; Lin, Y. C.; Ren, C. T.; Cheng, T. J.; Hsu, T. L.; Yu, A. L.; Wu, C. Y.; Wong, C. H. *Proc. Natl. Acad. Sci. U.S.A.* **2013**, *110*, 2517.
- (41) Miyaji, E. N.; Mazzantini, R. P.; Dias, W. O.; Nascimento, A. L.; Marcovitz, R.; Matos, D. S.; Raw, I.; Winter, N.; Gicquel, B.; Rappuoli, R.; Leite, L. C. *Infect. Immun.* **2001**, *69*, 869.
- (42) Godefroy, S.; Peyre, A.; Garcia, N.; Muller, S.; Sesardic, D.; Partidos, C. D. *Infect. Immun.* **2005**, *73*, 4803.
- (43) Stickings, P.; Peyre, M.; Coombes, L.; Muller, S.; Rappuoli, R.; Del Giudice, G.; Partidos, C. D.; Sesardic, D. *Infect. Immun.* **2008**, *76*, 1766.
- (44) Wu, T. N.; Lin, K. H.; Chang, Y. J.; Huang, J. R.; Cheng, J. Y.; Yu, A. L.; Wong, C. H. *Proc. Natl. Acad. Sci. U.S.A.* **2011**, *108*, 17275.
- (45) Cooper, N. R. *Adv. Immunol.* **1985**, *37*, 151.